The electronic spectrum of N-methylacetamide in aqueous solution: A sequential Monte Carlo/quantum mechanical study

4 AUTHORS, INCLUDING:

Willian R Rocha
Federal University of Minas Gerais

80 PUBLICATIONS **1,106** CITATIONS

SEE PROFILE

Kaline Coutinho
University of São Paulo

110 PUBLICATIONS **1,982** CITATIONS

SEE PROFILE

Sylvio Canuto
University of São Paulo

249 PUBLICATIONS **3,251** CITATIONS

SEE PROFILE

ELSEVIER

The electronic spectrum of *N*-methylacetamide in aqueous solution: a sequential Monte Carlo/quantum mechanical study

Willian R. Rocha [a], Katia J. De Almeida [b], K. Coutinho [c], Sylvio Canuto [d,*]

[a] *Núcleo de Estudos em Química Computacional (NEQC), Departamento de Química, ICE, Universidade Federal de Juiz de Fora, UFJF, 36036-330 Juiz de Fora, MG, Brazil*
[b] *Laboratório de Química Computacional e Modelagem Molecular (LQC-MM), Departamento de Química, ICEx, Universidade Federal de Minas Gerais, UFMG, 31270-901 Belo Horizonte, MG, Brazil*
[c] *Universidade de Mogi das Cruzes/CCET, CP 411, 08701-970 Mogi das Cruzes, SP, Brazil*
[d] *Instituto de Física, Universidade de São Paulo, CP 66318, 05315-970 São Paulo, SP Brazil*

Abstract

Sequential Monte Carlo/quantum mechanical (S-MC/QM) calculations are performed to study the solvent effects on the electronic transitions of *N*-methylacetamide (NMA) in aqueous solution. Full quantum mechanical INDO/CIS calculations are performed in the super-molecular clusters generated by Monte Carlo (MC) simulation. The largest calculation involves the ensemble average of 75 quantum mechanical results obtained with the NMA solute surrounded by 150 water solvent molecules. After extrapolation to the bulk limit we find that the $n \rightarrow \pi^*$ transition suffers a blue shift of 1755 cm^{-1} upon solvation and the $\pi \rightarrow \pi^*$ transition undergoes a red shift of 1180 cm^{-1}, in good agreement with the experimental findings. © 2001 Published by Elsevier Science B.V.

1. Introduction

The behavior of peptide groups (–CONH–) in aqueous solution has been of great interest for a long time. Peptide groups are the main repetitive units of polypeptide chains and proteins. Therefore, understanding how these groups can interact with each other and with the surrounding solvent molecules can give information about the native structures of proteins. The peptide group is also the main chromophore of proteins, which has a weak $n \rightarrow \pi^*$ transition at about 220 nm ($\sim$45 000 cm^{-1}) and a strong $\pi \rightarrow \pi^*$ transition at about 195 nm ($\sim$51 000 cm^{-1}). The electronic transitions of most side chains occur below 200 nm and are overpowered by the intense $\pi \rightarrow \pi^*$ transition of the peptide groups [1]. As a result, the electronic absorption spectroscopy of proteins in solution will resemble that of small peptide models in solution. For instance, the electronic spectra of random coil and β-strand proteins are very similar to peptide models as N,N-dimethylacetamide [1], with the $\pi \rightarrow \pi^*$ absorption being red shifted. However, the electronic spectrum of proteins having α-helix as the main secondary structure element looks quite different [2]. This feature has opened up an intense research field in which the electronic absorption spectroscopy is used to monitor the secondary structure patterns of proteins. In this case, the far-ultraviolet (UV) circular

* Corresponding author. Fax: +55-11-3818-6831.
E-mail address: canuto@if.usp.br (S. Canuto).

dichroism (CD) is the main technique [3]. Far-UV CD spectroscopy is a special kind of electronic absorption spectroscopy that uses circularly polarized light and the differences in left and right absorption of light are measured. The CD occurs only at energies where normal electronic absorptions take place and recently several theoretical works have appeared in which the normal electronic absorption spectra of small amide models have been studied, in order to furnish good parameters to improve the understanding of the far-UV CD spectra of proteins [4–7].

N-methylacetamide (NMA), $CH_3CONHCH_3$, is the simplest and classical model for the main chain of proteins. As a result, it has been extensively studied both experimentally and theoretically [4–23], attempting to understand how the intermolecular interactions between the clusters of NMA molecules and the interactions between the NMA with water can affect, for example, the structure, vibrational spectrum and rotational energy barrier.

Some of the theoretical investigations of the NMA molecule have focused on the structural, energetic and vibrational properties of NMA in gas phase and in aqueous solution (modeled mainly by continuum models or super-molecular approach). The theoretical study of the NMA electronic spectrum in solution is sparse. To the best of our knowledge the only theoretical study dealing with the solvent effects on the electronic spectra of NMA reported so far was due to Besley and Hirst [6] who performed a complete-active-space self-consisted-field employing the self-consistent-reaction-field approach to model the solvent. These same authors have reported more recently the electronic spectrum of NMA in solution, using the NMA–$(H_2O)_2$ complex embedded in a continuum dielectric [7]. They found that in order to model solvatochromic shift of the $n \rightarrow \pi^*$ transition, it may be necessary to consider more explicitly defined solvent molecules and many solvent configurations. It was also shown in this study that the $\pi \rightarrow \pi^*$ transition energy is little affected by the explicitly included solvent molecules, with the computed transition energy being very close to that obtained with the purely continuum solvent model. The peptide transition moment direction is crucial for predict-

ing the far-UV CD spectra of proteins and there are some interesting and complementary combined experimental/theoretical studies investigating the transition moment directions in amide single crystals. Clark [8] measured the polarized V–UV absorption spectra of single crystals of *N*-acetyl-glycine and found that the transition moments for the $n \rightarrow \pi^*$ and $\pi \rightarrow \pi^*$ transitions are polarized at −55 and −61°, respectively. INDO/S calculations showed a reasonable agreement with the experimental results. It was also shown by Clark that the crystal interactions do not lead to significant changes in the transition moment directions. More recently, Woody et al. [9] measured the single-crystal polarized reflection spectra of amides, with subsequent INDO/S calculations and concluded that the $\pi \rightarrow \pi^*$ transition dipole moment obtained by the INDO/S calculations is significantly different from experiment. These authors also proposed that in order to improve the calculation of the far-UV CD spectra of proteins the transition moment directions should be taken from ab initio calculations or experimentally for the isolated molecule, with the gas-to-crystal shifts taken from the INDO/S calculations. Since proteins are generally studied in a condensed phase, an understanding of the electronic spectrum of the constituent monomers in solution is very important.

In the present work, we deal with the electronic spectrum of NMA in an aqueous solution, using a sequential Monte Carlo/quantum mechanical (S-MC/QM) procedure [24–26]. We perform a systematic study of the solvent effects on the $n \rightarrow \pi^*$ and $\pi \rightarrow \pi^*$ electronic transitions of NMA, where the solvent molecules are explicitly included in the quantum mechanical calculations. This includes the electrostatic interaction between the solute and the solvent and the corresponding induced polarizations both in the solute and in the solvent. We use Monte Carlo (MC) simulations to generate structures of the liquid and super-molecular quantum mechanical calculations, with all-valence electrons, to obtain the separate contributions of the different solvation shells to the specific electronic transition. The largest calculation involves the ensemble average of 75 quantum mechanical results obtained with the NMA solute surrounded by as much as 150 water solvent molecules. At the

present stage, these super-molecular quantum mechanical calculations can only be made using semi-empirical methods. The quantum mechanical calculations start with a self-consistent-field intermediate neglect of differential overlap (INDO) calculation with a properly anti-symmetric wavefunction with 1230 valence electrons. The transition energies are obtained next using singly excited configuration interaction (CIS). The final result is estimated after extrapolation to the bulk limit. The S-MC/QM procedure differs from the conventional QM/MM in that all molecules – solute and solvent – are treated by quantum mechanics. The classical MC part is used only to generate the statistical structure of the liquid.

2. Theoretical methodology

MC statistical mechanics simulations are carried out employing standard procedures [27], including the Metropolis sampling technique and periodic boundary conditions using the minimum image method in a cubic box. The simulations are performed in the canonical (NVT) ensemble. The system consists of one NMA molecule plus 400 solvent molecules (water). The volume of the cubic box is determined by the experimental density of water, which at $T = 298.15$ K is 0.9966 g/cm^3. The intermolecular interactions are described by the standard Lennard–Jones plus Coulomb potential with three parameters for each atom i (ε_i, σ_i and q_i). For the water molecules we use the SPC potential developed by van Gunsteren and co-workers [28]. For NMA, we use the same potential of Jorgensen and Gao [20]. The intermolecular interactions are spherically truncated within a center of mass separation smaller than the cutoff radius, r_C, of 11.49 Å. Long-range corrections of the Lennard–Jones potential are calculated beyond this cutoff distance. In the simulation the molecules are kept with rigid geometries. The water molecules are kept in their C_{2v} structure with $r_{OH} = 1.000$ Å and $\angle HOH = 109.47°$. The NMA molecule is held rigidly in its structure, optimized at the MP2/6-31G(d) level of theory, as shown in Fig. 1. The initial configurations are generated randomly, considering the position and orienta-
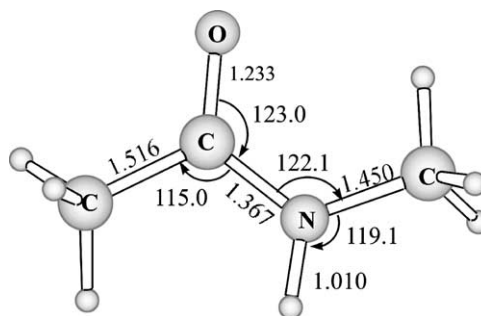

Fig. 1. Optimized (MP2/6-31G(d)) structural parameters for the NMA molecule. Distances in Å, angles in °.

tion of each molecule. A new configuration is generated after 400 MC steps, i.e., after all solvent molecules sequentially attempt to translate in all Cartesian directions and also attempt to rotate around a randomly chosen axis. The simulation consists of a thermalization phase of 2×10^6 MC steps, followed by an averaging stage of 24×10^6 MC steps. After completing the cycle over all 400 molecules a configuration is separated. Thus, the total number of configurations generated by the MC simulation is 60 000.

To analyze the solvent effects on the electronic spectra of the NMA molecule we employ the S-MC/QM procedure [24–26], in which the quantum mechanical calculations are performed on the super-molecular clusters, generated by the MC simulations, composed of one NMA and all solvent molecules within a particular solvation shell. To reduce the number of super-molecular clusters that will be submitted for the quantum mechanical calculations, the configurations are selected according to the auto-correlation function of the energy [25,26,29]. From this a total of 75 configurations are selected, with less than 5% of statistical correlation [24–26,29], and used in the quantum mechanical calculations. The solvation shells were defined from the analysis of the radial distribution function. The electronic spectra are then calculated using the semi-empirical ZINDO [30] program, within the INDO/CIS [31] approach. As the appropriate Boltzmann weights are included in the Metropolis Monte Carlo sampling technique, the average values of the transition energies and solvatochromic shifts are given as a

simple average over a chain of 75 uncorrelated configurations. The use of the auto-correlation function of the energy for selecting configurations has been shown before to be an efficient procedure for obtaining converged average values [29].

All ab initio calculations reported here were performed using the GAUSSIAN 98 program [32]. The MC statistical mechanics simulations were performed using the DICE program [33].

3. Results and discussions

3.1. Hydrogen bond

The MP2/6-31G(d) optimized structural parameters for the NMA molecule are shown in Fig. 1, which is in good agreement with the experimental structure obtained from electron diffraction experiments [13]. Fig. 2a shows the radial pair distribution function between the carbonyl oxygen of NMA and the water hydrogen, $g_{O-H}(r)$, as well as the radial distribution function between the carbonyl oxygen and the water oxygen, $g_{O-O}(r)$. Fig. 2b shows the radial distribution function between the amino hydrogen of NMA and the water oxygen, $g_{HO}(r)$. Hydrogen-bond interactions are obtained from the analysis of $g_{O-H}(r)$, $g_{O-O}(r)$ and $g_{H-O}(r)$ plots in Figs. 2a,b. The $g_{O-H}(r)$ and $g_{O-O}(r)$ distribution functions have sharp and well-defined first peaks, indicating a strong hydrogen-bond interaction. The first peak in the $g_{O-O}(r)$ distribution function starts at 2.35 Å, reaches its maximum at 2.27 Å and ends at 3.25 Å. For the $g_{O-H}(r)$, the first peak starts at 1.45 Å, passes through a maximum at 1.85 Å and ends at 2.55 Å. The spherical integration of the first peak in the $g_{O-O}(r)$ over the corresponding interval, gives 2.4 water molecules as nearest neighbors. The first peak of the $g_{H-O}(r)$ function starts at 1.55 Å, has a maximum at 1.95 Å and ends at 2.65 Å. After integration over this interval gives one water molecule as nearest neighbor.

Hydrogen bonds are also obtained using a geometric and energy criteria [26,34]. We consider a hydrogen-bond formation when the distance $R_{DA} \leqslant 4$ Å, the angle $\angle AHD \leqslant 30°$ and the binding energy are higher than 3.0 kcal/mol. In doing so, in the 75 MC configurations we find 120 hydrogen
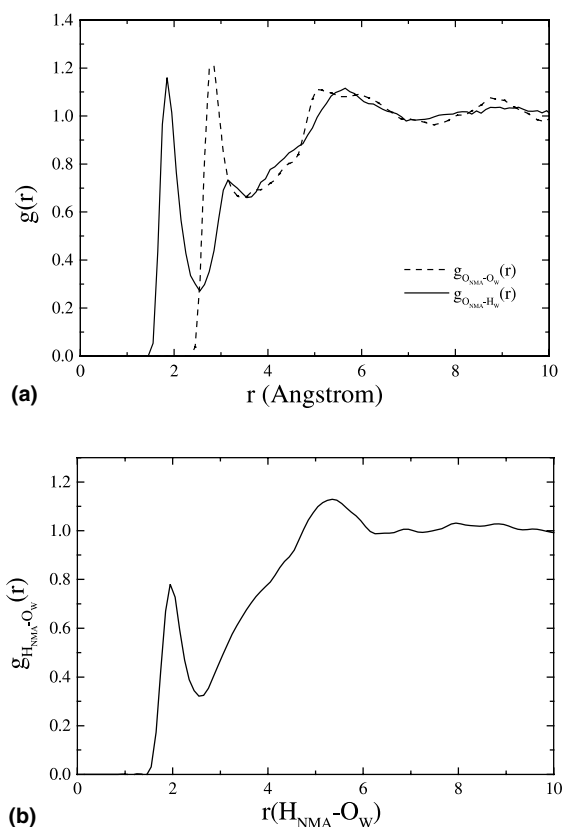

Fig. 2. Radial pair distribution function for the NMA in water system. (a) $g(r)$ between the carbonyl oxygen of NMA and the oxygen and hydrogen atoms of water. (b) $g(r)$ between the hydrogen atom of NMA (N–H) and the oxygen atom of water.

Table 1
Statistics of the hydrogen bonds formed between NMA and water and their contribution to the solvatochromic shifts of the $n \rightarrow \pi^*$ and $\pi \rightarrow \pi^*$ transitions[a]

Number of HB	Occurrence (%)	$n \rightarrow \pi^*$ shift (cm^{-1})	$\pi \rightarrow \pi^*$ shift (cm^{-1})
0	8	–	–
1	35	357	−404
2	47	673	−747
3	10	920	−1055
Total	100(120)	444 ± 27	−503 ± 26

[a] The calculated INDO/CIS transition energies, computed in gas phase, for the $n \rightarrow \pi^*$ and $\pi \rightarrow \pi^*$ transitions are, respectively, 35 004 and 56 620 cm^{-1}, with oscillator strengths of 0.001 and 0.236, respectively.

bonds formed in the oxygen site of NMA. This gives an average of 1.6 hydrogen bonds. NMA can form up to three hydrogen bonds with the surrounding water molecules and Table 1 gives the statistics obtained for the hydrogen bonds formed. We find that in 8% of the configurations the NMA does not form hydrogen bonds, 35% form one, 47% form two and 10% form three hydrogen bonds. The average value computed for the hydrogen-bonding energy when the carbonyl oxygen of NMA acts as a proton acceptor and when the NH group acts as a proton donor are −5.6 and −4.8 kcal/mol, respectively. Typical hydrogen-bonded structures obtained in the simulation are shown in Fig. 3.

3.2. Electronic spectrum

Table 2 summarizes some experimental results obtained for the $n \to \pi^*$ and $\pi \to \pi^*$ electronic
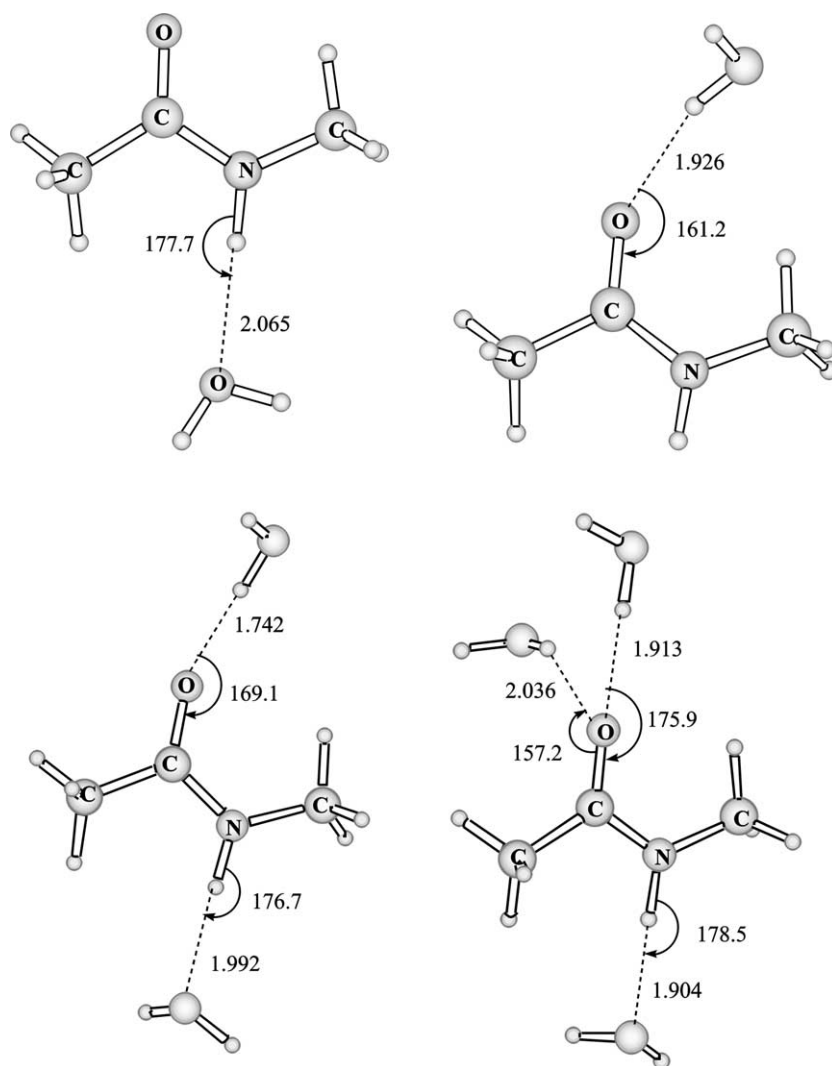

Fig. 3. Typical hydrogen-bonding interactions between the NMA molecule and water, obtained during the simulation. Distances in Å, angles in °.

Table 2
Summary of the experimental results for the absorption transitions of NMA in gas phase and in solution

Band assignment	Experimental					
	Gas phase[a]		Water[b]		Cyclohexane[b]	
	Energy (cm^{-1})	f	Energy (cm^{-1})	f	Energy (cm^{-1})	f
$n \rightarrow \pi^*$	N/A[c]	N/A[c]	44 683	0.0025	44 683	0.0025
$\pi \rightarrow \pi^*$	54 926	N/A[c]	53 797	0.300	54 361	0.170

[a] Vacuum measurements, taken from [11].
[b] Ref. [12].
[c] Not available.

transitions of NMA molecule in gas phase, water and in cyclohexane. As it can be seen, the $\pi \rightarrow \pi^*$ transition undergoes a red shift of 1130 cm^{-1} on going from the gas phase to the aqueous solution. The $n \rightarrow \pi^*$ transition is not measured in the gas phase and so, we cannot estimate the corresponding experimental solvatochromic shift of this transition. We could, in principle, assume that the results obtained in cyclohexane are the same as of those for the gas phase, however, recent experimental work has shown that NMA tends to self-associate in apolar solvents [35], invalidating this assumption.

The calculated solvatochromic shifts on the electronic transitions of NMA, due only to the hydrogen bonds between the NMA and water, are shown in Table 1. The $n \rightarrow \pi^*$ transition of NMA suffers a blue shift of 444 cm^{-1} due only to hydrogen-bonding interactions. Similarly, the $\pi \rightarrow \pi^*$ undergoes a red shift of 503 cm^{-1}. To analyze the effect of the outer solvation shells on the electronic transitions of NMA, we use the solvation shells around the NMA molecule, defined from the radial distribution function $(g(r))$ considering the center-of-mass (cm) of the solute and solvent molecules. The $g_{cm-cm}(r)$ calculated for the NMA molecule in water solution is depicted in Fig. 4, where two solvation shells are easily distinguished. The first solvation shell starts at 2.85 Å and extends up to 4.45 Å. The second solvation shell ends at 6.55 Å. Spherical integration of the $g_{cm-cm}(r)$ over the corresponding intervals gives 8 and 36 water molecules in the first and second solvation shells, respectively. Since the liquid is not structured beyond the second solvation shell, we just added

more solvent molecules up to 150 and we named these shells as third, fourth and so on. For each shell a total of 75 quantum mechanical calculations of the electronic spectrum were performed and the values of the transition energies were averaged out. The results obtained are reported in Table 3. Our largest calculation, made for the outermost shell, includes one NMA molecule and 150 water molecules, with a total of 1230 valence electrons explicitly included. The corresponding calculated shifts for the $n \rightarrow \pi^*$ and $\pi \rightarrow \pi^*$ transitions of NMA are 1362 and -998 cm^{-1}, respectively. The results of Table 3 show that water molecules located beyond 10 Å can still influence the solvation shift. This is a consequence of the increased dipole moment of the complex formed by the hydrogen bond between the solute and the solvent. The monotonic behavior of the calculated energy shift for the $n \rightarrow \pi^*$ and $\pi \rightarrow \pi^*$ transitions of NMA
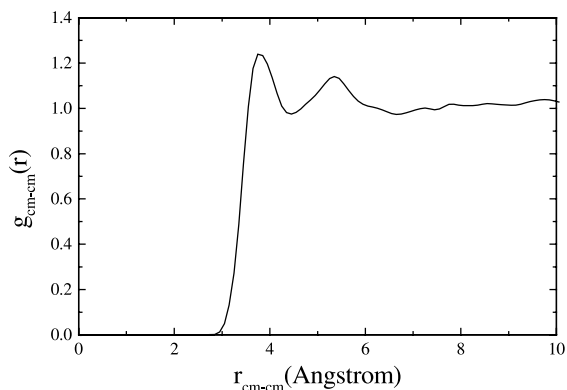

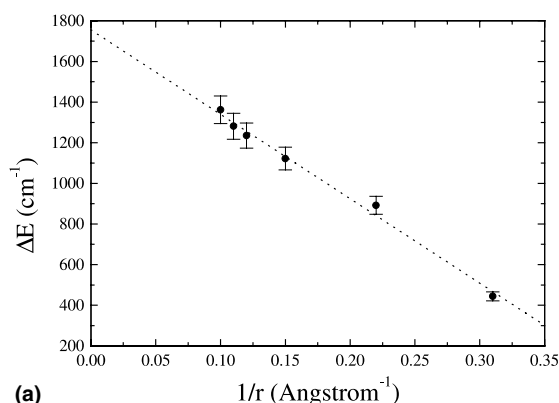Fig. 4. Radial pair distribution function between the NMA and water.

Table 3
Variation of the calculated (INDO/CIS) shifts of the $n \rightarrow \pi^*$ and $\pi \rightarrow \pi^*$ transitions of NMA in water with the solvation shells

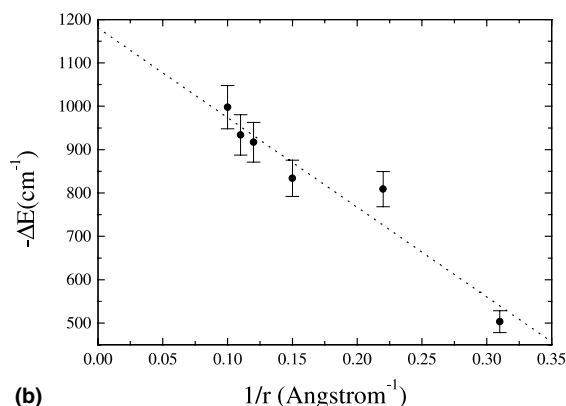| Solvation shell	N	M	L	r (Å)	$n \rightarrow \pi^*$ shift (cm^{-1})	$\pi \rightarrow \pi^*$ shift (cm^{-1})
First	8	94	75	4.45	892 ± 43	-809 ± 46
Second	36	318	75	6.55	1122 ± 51	-834 ± 52
Third	74	622	75	8.20	1235 ± 51	-917 ± 49
Fourth	100	830	75	9.05	1281 ± 51	-934 ± 52
Fifth	150	1230	75	10.3	1362 ± 50	-998 ± 47
Limit	Bulk				1755 ± 50	-1180 ± 60
Experimental					N/A	-1130

N is the total number of water molecules included. M is the total number of valence electrons included in the quantum mechanical calculations. L is the number of MC configurations used for ensemble average. r is the radius of the solvation shell obtained from the radial distribution function shown in Fig. 4. Experimental result is taken from Table 1. N/A means the result is not available.

permits an extrapolation of the results to the bulk limit. In doing so, we obtain a limiting value of 1755 and -1180 cm^{-1} for the $n \rightarrow \pi^*$ and $\pi \rightarrow \pi^*$

(a)

(b)

Fig. 5. Calculated solvatochromic shift for the $n \rightarrow \pi^*$ (A) and $\pi \rightarrow \pi^*$ (B) transition of NMA in water, as a function of the inverse size of the solvation shell as shown in Table 3.

transitions, as can be seen in Fig. 5. This would be our best estimate for the solvatochromic shifts of the $n \rightarrow \pi^*$ and $\pi \rightarrow \pi^*$ electronic transitions of NMA in aqueous solution. This final value for the $\pi \rightarrow \pi^*$ transition is in excellent agreement with the experimental observations. Unfortunately we do not have an experimental estimate for the $n \rightarrow \pi^*$ electronic transition of NMA, maybe due to the broad aspect of the $\pi \rightarrow \pi^*$ transition, in conjunction with the very low intensity of the $n \rightarrow \pi^*$ transition. However, it is interesting to see that the solvation shifts are affected by long-range polarizations extending beyond 10 Å, and we must go to the outer solvation shells to reproduce the experimental results for $n \rightarrow \pi^*$ transitions shifts [26].

4. Summary and conclusions

In this work, we employed an S-MC/QM procedure to analyze the solvent effects on the $n \rightarrow \pi^*$ and $\pi \rightarrow \pi^*$ electronic transitions of NMA in aqueous solution. The structural analysis of the solution, by means of the radial pair distribution function, showed that NMA can form up to three hydrogen bonds with water. The hydrogen bond statistics revealed that in 8% of the configurations the NMA does not form hydrogen bonds with water, 35% form one, 47% form two and 10% form three hydrogen bonds. The average values computed for the hydrogen bond energies when the carbonyl oxygen of NMA acts as a proton acceptor and when the NH group acts as a proton

donor were -5.6 and -4.8 kcal/mol, respectively. The $n \to \pi^*$ transition of NMA suffers a blue shift of 444 cm^{-1} due only to hydrogen-bonding interactions. Similarly, the $\pi \to \pi^*$ undergoes a red shift of 503 cm^{-1}. Next, 75 quantum mechanical calculations were made for each of the first, second and outer solvation shells up to the limit of 150 water molecules. The variation of the spectral shift with the solvation shells showed that the solvation shifts are affected by long-range polarizations extending beyond 10 Å. After extrapolation to the bulk limit we found that the $n \to \pi^*$ transition suffers a blue shift of 1755 cm^{-1} upon solvation and the $\pi \to \pi^*$ transition undergoes a red shift of 1180 cm^{-1}. The latter result is in good agreement with the experimental result of 1130 cm^{-1}. The calculations of the far-UV CD spectra were not the main concern of this work but, maybe it should be interesting to use the experimental transition moment directions in conjunction with the gas-to-liquid solvatochromic shifts reported here, to test if any improvement is achieved on the CD calculations. Further studies on the preferential solvation of NMA in binary mixtures and how the intermolecular interactions affect the electronic spectrum are in progress.

Acknowledgements

References

[1] K.E. van Holde, W.C. Johnson, P.S. Ho, Principles of Physical Biochemistry, Prentice-Hall, New Jersey, 1998.
[2] K. Rosenheck, P. Doty, Proc. Natl. Acad. Sci. USA 47 (1961) 1775.
[3] R.W. Woody, Methods Enzymol. 246 (1995) 34.
[4] J.D. Hirst, J. Chem. Phys. 109 (1998) 782.
[5] R.W. Woody, N. Sreerama, J. Chem. Phys. 111 (1999) 2844.
[6] N.A. Besley, J.D. Hirst, J. Phys. Chem. A 102 (1998) 10 791.
[7] N.A. Besley, J.D. Hirst, J. Mol. Struct. Theochem. 506 (2000) 161.
[8] L.B. Clark, J. Am. Chem. Soc. 117 (1995) 7974.
[9] R.W. Woody, G. Raabe, J. Fleischhauer, J. Phys. Chem. A 103 (1999) 8984.
[10] G. Sieler, R. Schweitzer-Stenner, J. Am. Chem. Soc. 119 (1997) 1720.
[11] K. Kaya, S. Nagakura, Theor. Chim. Acta 7 (1967) 124.
[12] E.B. Nielsen, J.A. Schellman, J. Phys. Chem. 71 (1967) 2297.
[13] M. Kitano, Y. Fukuyama, K. Kuchitsu, Bull. Chem. Soc. Jpn. 46 (1973) 384.
[14] F. Fillaux, C. De Lozé, Chem. Phys. Lett. 39 (1976) 547.
[15] R. Schweitzer-Stenner, G. Sieler, N.G. Mirkin, S. Krimm, J. Phys. Chem. A 102 (1998) 118.
[16] H. Torii, T. Tatsumi, T. Kanazawa, M. Tasumi, J. Phys. Chem. B 102 (1998) 309.
[17] K. Guo, M. Karplus, J. Phys. Chem. 98 (1994) 7104.
[18] W. Han, S. Suhai, J. Phys. Chem. 100 (1996) 3942.
[19] R. Ludwig, F. Weinhold, T.C. Farrar, J. Phys. Chem. 101 (1997) 8861.
[20] W.L. Jorgensen, J. Gao, J. Am. Chem. Soc. 110 (1988) 4212.
[21] V.L. Furer, J. Mol. Struct. 435 (1997) 151.
[22] J.D. Hirst, D.M. Hirst, C.L. Brooks III, J. Phys. Chem. A 101 (1997) 4821.
[23] L. Serrano-Andrés, M.P. Fülscher, J. Am. Chem. Soc. 118 (1996) 12 190.
[24] K. Coutinho, S. Canuto, Adv. Quantum Chem. 28 (1997) 89.
[25] K. Coutinho, S. Canuto, M.C. Zerner, J. Chem. Phys. 112 (2000) 9874.
[26] S. Canuto, K. Coutinho, Int. J. Quantum Chem. 77 (2000) 192.
[27] M.P. Allen, D.J. Tildesley, Computer Simulation of Liquids, Oxford University Press, Oxford, 1987.
[28] H.J.C. Berendsen, J.P.M. Postma, W.F. van Gunsteren, in: B. Pullman (Ed.), Intermolecular Forces, Reidel, Dordrecht, 1981, p. 331.
[29] W.R. Rocha, K. Coutinho, W.B. De Almeida, S. Canuto, Chem. Phys. Lett. 335 (2001) 127.
[30] M.C. Zerner, ZINDO: A Semi-empirical Program Package, University of Florida, Gainesville, FL 32611.
[31] J. Ridley, M.C. Zerner, Theor. Chim. Acta 32 (1973) 111.
[32] M.J. Frisch, et al., GAUSSIAN 98, Revision A.6, Gaussian, Inc., Pittsburgh, PA, 1998.
[33] K. Coutinho, S. Canuto, DICE: A Monte Carlo Program for Liquid Simulation, University of São Paulo, São Paulo, 1997.
[34] W.L. Jorgensen, J. Chandrasekhar, J.D. Madura, R.W. Impey, M.L. Klein, J. Chem. Phys. 79 (1983) 926.
[35] M. Akiyama, H. Torii, Spectrochim. Acta Part A 56 (1999) 137.